EP-1890: Accurate organs at risk contour propagation in head and neck adaptive radiotherapy

Zhai, T.T.; Bijl, H.P.; Langendijk, J.A.; Steenbakkers, R.J.; Brouwer, C.L.; Laan-Boomsma, H.J. Van der; Sijtsema, N.M.; Kierkels, R.G.

DOI:
10.1016/S0167-8140(16)33141-3

Conclusion: Automated segmentation of the pancreas with accuracy useful for organ motion tracking is achieved based on T1 weighted VIBE images. Automated pancreas segmentation based on T2 weighted HASTE images is not as robust. Considering the segmentation accuracy, levels of human supervision and computational speed, dictionary learning is the preferred segmentation method for real time MRI pancreas segmentation.

EP-1888

Accuracy and limitations of deformable image registration with SmartAdapt® in the thorax region

S. Sarudis[1], A. Karlsson Hauer[2], D. Bibac[3], A. Bäck[2]
[1]*Sahlgrenska University Hospital, Therapeutic Radiation Physics, Borås, Sweden*
[2]*Sahlgrenska University Hospital, Therapeutic Radiation Physics, Gothenburg, Sweden*
[3]*Södra Älvsborgs Sjukhus, Diagnostic Imaging and Laboratory Medicine, Borås, Sweden*

Purpose or Objective: Systematically determine the accuracy and limitations of the deformable image registration (DIR) algorithm in SmartAdapt® and present a workflow which minimises the errors and uncertainties in a deformation process.

Material and Methods: Deformable image registrations were performed on 4-dimensional computed tomography (4DCT) scans of a dynamic thorax phantom (CIRS, 008A) and patients with lung tumours that did a 4DCT scan within their regular preparation procedure before receiving external beam radiation therapy. To evaluate the performance of the DIR algorithm, the tumour in the phantom and the organs of interest for each patient (tumour, lungs, heart and spinal cord) were manually delineated in each breathing phase of the 4DCT, and the Centre of Mass Shift (CMS) and Dice Similarity Coefficients (DSC) between the deformed and manually delineated target volumes were calculated. Target shifts between 0 - 53 mm and absolute volumes between 0.5 - 1600 cm3 were evaluated. The phantom scans were repeated twice with image thicknesses of 1 and 3 mm to determine the impact on the deformation accuracy. All deformations were performed using SmartAdapt® v11.0.

Results: Target motion and volume changes are generally reproduced with CMS agreement of <2 mm and DSC >0.90. However large failures in deformed target volumes may occur when the target position is adjacent to voxels with the same intensity as the voxels within the target, if the volume of interest is set too small or if the target shift is large relative to its absolute volume. In these cases the DSC may decrease to zero meaning there is no overlap in any point between the deformed and the true target volumes. In general, the deformation accuracy decreases as the complexity and the image thickness increases. The deformed volumes may vary in shape and position between individual deformations even though all parameters in the deformations process are kept constant. Visual verification of the deformed volume before approval is therefore crucial to keep the accuracy as high as possible.

Conclusion: In general, SmartAdapt® offers a useful tool for DIR with CMS agreement of <2 mm and DSC >0.90 between the deformed and the manually delineated target volumes. More complex deformations containing large relative changes in target volume and position are less accurate with DSC decreasing to zero. Every deformation process should be repeated until visual inspection of the deformed volume is satisfactory in order to keep the accuracy as high as possible.

EP-1889

Quality assurance of image registration algorithms using synthetic CT/MRI/PET datasets

A. Perez-Rozos[1], M. Lobato Muñoz[1], I. Jerez Sainz[1], J. Medina Carmona[2]
[1]*Hospital Virgen de la Victoria, Radiation Oncology. Medical Physics., Malaga, Spain*
[2]*Hospital Virgen de la Victoria, Radiation Oncology, Malaga, Spain*

Purpose or Objective: To develope a method to generate synthetic datasets to perform quality assurance of multimodality registration algorithms.

Material and Methods: Relevant geometries, resembling phantoms and human body, are generated using in-house software and PENGEOM (PENELOPE) routines to represent clinically relevant situations. Every region of interest is characterized using user defined parameters: material density, uptake index parameter, T1, T2 and proton density parameters. Using these parameters and geometry it is possible to generate three datasets: synthetic-CT dataset, a synthetic-PET dataset, and a synthetic-MRI dataset. For synthetic CT Hounfield units are assigned using material density and a standard calibration curve; for synthetic PET SUV values are assigned using uptake index parameter for every ROI and then applying a gaussian blur filter to mimic PET resolution; synthetic MRI signal values are assigned using T1, T2, proton density and repetition and echo times using parametrization formulas that calculate signal values for T1, T2 or proton weighted sequences. Known rotations, shifts, and deformations can be applyed to every dataset. The different datasets could be imported in treatment planning systems as usual and then apply the registration and fusion algorithms, that would have to recalculate the previously applied rotations and shifts.

Results: In the image we show an example of a mathematical phantom with a cortical bone ring, soft tissue with three spheres and two parallelepiped regions. Some regions are visible only in PET or MRI datasets. In lower part of image it is shown an example of PET image shift and rotation and the corresponding CT-PET image registration.

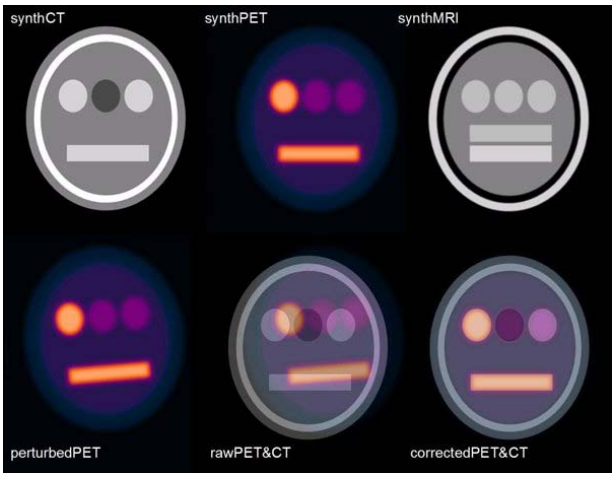

Conclusion: Use of synthetic datasets allows for comprehensive quality assurance of registration algorithms of several systems used in radiation therapy.

EP-1890

Accurate organs at risk contour propagation in head and neck adaptive radiotherapy

T.T. Zhai[1,2], H.P. Bijl[2], J.A. Langendijk[2], R.J. Steenbakkers[2], C.L. Brouwer[2], H.J. Van der Laan-Boomsma[2], N.M. Sijtsema[2], R.G. Kierkels[2]
[1]*Cancer Hospital of Shantou University Medical College, Department of Radiation Oncology, Shantou, China*
[2]*University of Groningen- University Medical Center Groningen, Department of Radiation Oncology, Groningen, The Netherlands*

Purpose or Objective: Adaptive radiotherapy for head and neck cancer patients aims to correct for geometrical changes due to tumour shrinkage, mucosal swelling and weight loss. These changes are monitored by weekly acquired repeat CT scans (rCTs) on which the actual treatment plan is evaluated.

The resulting large workload requires automated contour propagation from planning CT (pCT) to the rCTs. Consequently, decisions to re-plan are directly based on the propagated contours. Therefore, we investigated whether deformable propagated organs at risk (OARs) contours of head and neck cancer patients can be used for clinical treatment plan evaluation on rCTs.

Material and Methods: Planning CTs and weekly acquired rCTs of ten head and neck cancer patients were included in the analysis (in total: 10 pCTs and 67 rCTs). The following OARs were delineated on each pCT: parotid glands, submandibular glands, pharyngeal constrictor muscle, cricopharyngeal muscle, oral cavity, mandible, thyroid, supraglottic larynx, glottic area, and spinal cord. Hence, the transformation between each rCT and pCT was derived using an intensity based deformable image registration algorithm. The transformation was used to automatically propagate all contours to the rCTs (AC). All propagated contours were evaluated by an expert and corrected if necessary (corrected contours: CC). To validate deformable contour propagation for treatment plan evaluation, the AC and CC were compared by the Dice Similarity Coefficient (DSC). The AC to CC contour distances were evaluated using the combined gradient of the distance transform (ComGrad) method. Furthermore, dosimetric parameters were compared.

Results: The ACs were very similar to the CCs with an average (±SD) DSC for all structures of 0.93 ± 0.07 (range: 0.57-1.00), indicating no or minor corrections required for the majority of contours. The DSC was lower than 0.8 for 10% of the pharyngeal constrictor muscle and 12% of the cricopharyngeal muscle contours, respectively. For all other structures the DSC was larger than 0.9 for 93% of the contours. The average 90th percentile AC to CC contour distance was below the size of an image voxel (0.66 ± 0.25 mm; range: 0.00 - 1.50 mm). The dosimetric parameters revealed only small differences between the AC and CC dose values. Only in 3% of all analyzed contours the difference in accumulated dose between the AC and CC was more than 2 Gy. In Figure 1 the fractional ipsilateral parotid gland dose of AC and CC is shown for five representative cases.

Figure 1. The fractional mean dose of the automated (AC) and corrected (CC) ipsilateral parotid gland contours of 5 patients

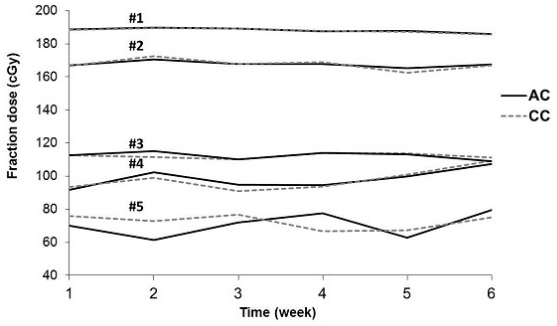

Conclusion: Deformable OARs contour propagation from the planning CT to weekly acquired repeat CTs in the head and neck area resulted in similar contours and dosimetric values compared to the ground truth manually corrected contours. Only smaller contours such as the swallowing muscles, required manual review when used for decision making on replanning. Automatic contour propagation makes it feasible to include more patients in an adaptive radiotherapy schedule.

EP-1891

Determination of physical body outline in relation to outline visualisation in MRI for RT planning

S. Weiss[1], M. Helle[1], S. Renisch[1]
[1]*Philips GmbH Innovative Technologies, Research Laboratories, Hamburg, Germany*

Purpose or Objective: The geometric accuracy of MR-only based RT planning is influenced by several aspects, most of which have been evaluated thoroughly and solutions been provided: differently shaped MR and treatment tables, skin indentations by MR coils, geometrical distortions in MRI, and accuracy of segmentation. This work evaluates whether the body outline as visualized by MRI precisely matches the physical body outline, or whether there is potentially any skin layer that is not visualized by MRI. Correct delineation of the body outline is important because it directly influences attenuation and hence dose delivered to treatment and risk organs.

Material and Methods: Standard ultra-sound gel was doped with 10% Gd-contrast agent, and a lump of gel was applied to the thigh of a male volunteer. Two polyethylene foils (50µm and 12µm thickness) were immersed in doped gel in a phantom and located beside the gel on the thigh to serve as a reference. A two-channel surface coil (diameter 7cm) was used to acquire axial images with a 3D T1w-FFE-mDIXON sequence as used for MR-only RT planning in prostate. Images were acquired at standard resolution (1.7mm²x2.5mm) and high resolution (0.5mm²x2mm) in a 200mm²x10mm FOV on a 1.5T scanner (Philips Achieva). Read-out was chosen in LR direction to avoid any water-fat shift perpendicular to the skin.

Results: None of the reconstructed images (TE1, TE2, water, in-phase, opposed-phase) revealed any hypo-intense layer between the outermost MR-visible layer and the gel (c.f. Fig: thin white arrows). However, the 50µm PE foil in the phantom was clearly visible in the highly resolved images (bold white arrows), and the 12µm foil was just about visible (bold grey arrows). Initial scans had shown that plain gel generates a much stronger signal than the outer skin layer, so that the gel signal obscures the skin signal, which complicates image interpretation. Doping with 10% contrast agent resulted in a match of signal strength of gel and skin and resolved this. Image interpretation was unambiguous with respect to water-fat shift, since it was chosen parallel to the skin surface in the evaluated region.

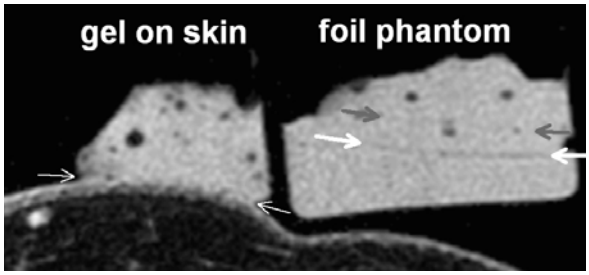

Conclusion: It can be concluded that any MR-invisible skin layer that may be present on top of the outermost MR-visible layer but not be visualized due to lack of free water or other MRI effects has a thickness of less than 20µm. Such a thin layer would have a negligible effect on simulation of attenuation maps and respective dose planning, which is clinically done with a spatial resolution of 4mm.

EP-1892

Using deformable image registration to integrate diagnostic MRI into the planning pathway for HNSCC

R. Chuter[1,2], R. Prestwich[3], A. Scarsbrook[1], J. Sykes[4], D. Wilson[1], R. Speight[1]
[1]*St James's University Hospital, Medical Physics and Engineering, Leeds, United Kingdom*
[2]*The Christie, Medical Physics and Engineering, Manchester, United Kingdom*
[3]*St James's University Hospital, Clinical Oncology, Leeds, United Kingdom*
[4]*University of Sydney, Institute of Medical Physics, Sydney, Australia*

Purpose or Objective: To assess the accuracy of Gross Tumour Volume (GTV) delineation for head and neck